

WRINKLING STRESSES IN HONEYCOMB SANDWICH PANELS USING DISCRETE AND CONTINUUM CORE REPRESENTATIONS

R.A Staal¹, D.P.W Horrigan², G.D Mallinson³,

1. Air New Zealand Ltd, P.O Box 53098, Auckland International Airport, Auckland, New Zealand
2. TASS Inc. 12016 115th Ave NE Suite 100, Kirkland, WA 98034
3. Department of Mechanical Engineering, University of Auckland, Private Bag 92019, Auckland, New Zealand

ABSTRACT

This study, examines the implications of modeling wrinkling in sandwich honeycomb cores using a simplified continuum representation of the core. Localised wrinkling in sandwich honeycomb panels is traditionally modeled using a continuum core. In a continuum core, the support provided to the facesheet is constant, while in reality it is discrete with cellular core. Classical linear wrinkling expressions, based on this continuum core assumption over predict the observed stresses. This paper aims to assess whether the method of representing the core causes this discrepancy, or whether there are other reasons for this difference. The problem is reviewed using a series of linear finite element models. One model is based on cellular core, while the other is based on a continuum core. Properties used in the continuum model are directly extracted from the discrete finite element model. Direct comparisons are made between the two linear buckling loads. Comparisons are also made between existing analytical models and continuum finite element models. It is shown that both types of models predict the same wrinkling stress, providing accurately converted properties are used.

Keywords: wrinkling, discrete core, continuum core, honeycomb, sandwich panel

1. INTRODUCTION

Sandwich panels are used extensively on modern commercial aircraft for fuselage fairings, engine cowlings, internal floor panels and flight control surfaces, in marine applications and transportation in general. One drawback of sandwich construction and composite materials is they exhibit a large number of failure modes, most of which are hard to predict. Wrinkling is one of these failure mechanisms. This is localised failure that is predominant in sandwich panels with thin face sheets and honeycomb cores.

Wrinkling is a localised instability consisting of wavelengths smaller than the overall face length and occurs in panels that are subject to an in-plane compressive load in the face sheet, which can be through either bending or axial compression. It is controlled by the vertical support provided by the core to the facesheet and the shear stiffness of the core. This support governs the wrinkling wavelength and the buckling load.

Various models [1-5] have been developed to predict the onset of wrinkling in sandwich structures. Most are based around linear buckling extractions and assume that the core provides continuous support to the facings (continuum core representation). Most of these models have led to the same result in regards to the predicted wrinkling stresses and the derivation [1]. The general expressions for wrinkling stress in an isotropic sandwich beam under plane stress is given by Hoff and Mautner [2] as:

$$\sigma_{cr} = C(E_f E_c G_c)^{\frac{1}{3}} \quad (1)$$

The value of C changes depending on the decay function and depth of the wrinkle. The traditional model of Hoff and Mautner [2] used a linear decay function which gave a C value of 0.91. Plantema [1] used an exponential decay function which results in a value of C of 0.85 for a plate and 0.825 for a thin beam. Gough and Bruyne [3] found a C of

0.78. Allen [4] and Zenkert [5] also calculated a value of C of 0.78 using Airy stress functions. Staal [6] used equilibrium conditions to calculate the decay function. This led to the same coefficient as Plantema of 0.825. It should be noted that these models are independent of length scales, i.e depend only on material properties. This is a valid assumption when $t_c/t_f > 17$ or when no subsurface damage exists as presented in Staal et al [7].

For a more detailed review of wrinkling models refer to the work by Zenkert [5] and Staal [6]. For the purpose of this study a coefficient of 0.825 will be used for future comparisons.

Unfortunately, these models tend to over predict failure loads. During experiments, the panels fail at about 60% of the predicted wrinkling load from the linear models [2]. This discrepancy has previously been attributed to imperfections and irregularities in the structure.

This paper reconsiders the underlying continuous core support assumption in respect to wrinkling failure. Using a simplified continuum core, to model a strictly discrete structure, could lead to differences between linear wrinkling models and experimental results. Wrinkles form at a natural wavelength – for Nomex® honeycomb type cores the wavelength approaches one cell per wrinkle. For honeycomb cores it is possible that cells could have an influence on the buckling load and mode. The objective of this paper is to determine if continuum cores can be used to model wrinkling failure in honeycomb panels. Due to the complexity of the cellular geometry, this is completed using a Finite Element (FE) package.

2. DEVELOPMENT OF CONTINUUM AND DISCRETE FINITE ELEMENT MODELS

The paper compares the wrinkling stresses of a discrete cellular model with a continuum solid model. This relatively straightforward procedure consists of developing discrete-core FE model and continuum-core FE model (using continuum properties calculated from the discrete finite element model, Figure 1) and comparing their linear buckling loads.

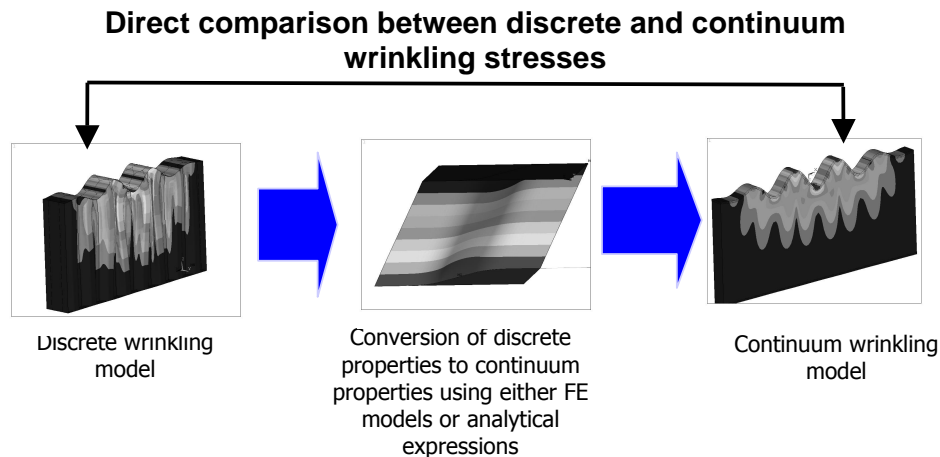


Figure 1: Method used to compare of discrete and continuum wrinkling models

2.1. Discrete finite element model

The discrete model consists of individual cells, faces and end plates modeled using shell elements. Figure 2 and Figure 3 show a typical discrete cell FE model.

The core consists of a number of cells made from shell walls, linked together to form hexagonal shapes. Attached to the top and bottom of the core is another shell wall that represents the face. At either end of the core are two more shell faces, used for constraints and loading surfaces. All shell faces are attached by coincident nodes.

Loads are applied through a pure varying pressure load on one end-plate and a fixed constraint on the other end-plate. The varying pressure load puts the panel into pure bending and the upper facesheet into in-plane compression.

The walls in line with the ribbon direction, are double the thickness of the angled walls (see Figure 2). This is consistent with actual honeycomb cores. The walls are assigned the modulus of the parent core material and the faces are assigned isotropic properties, as the fibre orientation has not been modelled and it has been assumed that the lay-up is symmetrical in the principle orientations. The sandwich panel is symmetric about its centre line, with both faces being assigned the same thickness.

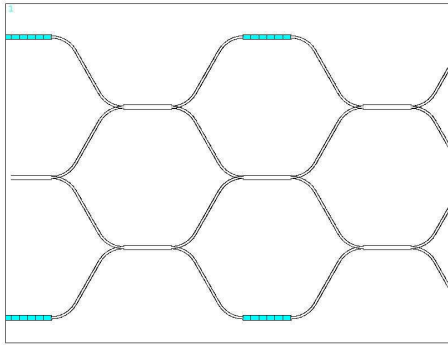


Figure 2: Plan view of the cells showing double wall thicknesses in the line with the ribbon or X direction

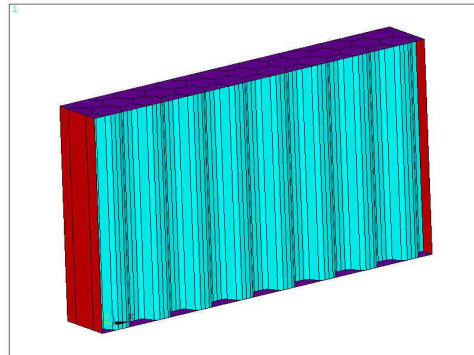


Figure 3: Typical Discrete FE model consisting of 8 cells in the ribbon direction and 2 cells in the transverse direction and fillets in the junctions

Symmetry constraints were used on either side of the discrete model to reduce the number of cells in the transverse direction. To compare discrete to continuum models directly the same restraints and boundary conditions were used on the continuum model. All wrinkling models were solved using an eigenvalue solver. Symmetry constraints were used down the sides of the core to reduce the number of cells in the transverse direction and to mimic the behavior of an infinitely wide structure.

At least eight cells were used in the ribbon direction to allow a complete wrinkle to form in the facings. The element density and the number of cells in the discrete core were verified in a convergence study.

Fillets were added at the intersection of the cellular walls, to represent the fillets in actual nomex core (Figure 2). When a straight walled joint was initially used, the model tended to wrinkle adjacent to the joint and produce a false result. This was due to the geometric stiffness of the straight wall junction. When fillets were used the structure buckled in the top facesheet, at approximately twice the stress predicted by the straight-walled model. This stress and mode were verified using a non-linear buckling solution.

The majority of the models were set up with the parameters in Table 1. These values were established during a convergence study that found the best combinations of cell numbers and element density that gave the best results in terms of solution and solving time.

| Parameters | |
|------------------------------------|----|
| Number of cells (ribbon direction) | 8 |
| Number of cells (width direction) | 1 |
| Mesh density (height) | 15 |
| Mesh density (cell wall length) | 7 |

Table 1: Standard parameters used in the discrete model

2.2. Continuum finite element model

The continuum panels were modeled with a combination of shell and solid elements. Shell elements were used for the faces and loading plates on each end of the panel. Twenty-noded brick elements with a reduced integration element formulation were used to model the core.

The continuum model was constrained and loaded in the same way as the discrete model, with a varying pure pressure load on one end and a fixed constraint on the other. Symmetry constraints were used on the side walls.

For completeness, a plane stress model was also developed for comparison purposes.

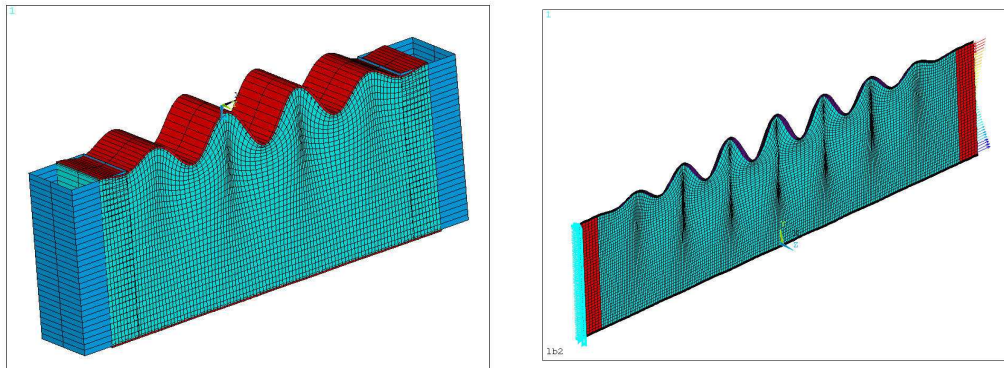


Figure 4: Continuum 3D solid model showing linear buckled shape and un-deformed shape

2.3. Equivalent continuum honeycomb core properties

There are two types of properties required in the continuum models; out-of-plane and in-plane. Out-of-plane properties are those properties that act in the through thickness direction (G_{xz} , G_{yz} , E_z) while in-plane properties (E_x , E_y) act in-line with the sandwich panel.

The out-of-plane properties are the most important for the functionality of the core, as they resist the shear stresses and out-of-plane loading.

The in-plane properties are usually ignored completely as the core is considered to have negligible stiffness in the X and Y planes and all of the in-plane compression and tensile

forces are carried by the faces. This is a reasonable assumption for the majority of failure modes and global deflections, but is insufficient when predicting local wrinkling failure. With wrinkling the in-plane stiffness prevents the core from bowing outwards as wrinkles form in the facings. With low in-plane core stiffness the panel will tend to wrinkle even at low loads.

When most authors (e.g Ashby and Gibson [8], Burton and Noor [9] & Vonach and Rammerstorfer [10]) have considered the in-plane modulus, they have considered it in a free state (when the core has no facesheets attached to each surface). Without facesheets the core is like a large spring and has about 1000th of the stiffness of the out-of-plane directions.

When a face sheet is bonded to the core, the cellular walls must have the same deformation as the face sheet. Because the surfaces of the core are restrained, the side walls must have the same displacement as the face sheet (shown in Figure 5), thereby altering the problem from one of pure bending, to a combination of extension and bending. This additional restraint can have a marked effect on the effective in-plane stiffness of the core. For example, for small cell Nomex cores such as HRH10-1/8"-3, the in-plane modulus can change from a unrestrained state value of 0.15 MPa to the restrained state value of 3 MPa, an increase of approximately 20 times. These values are extracted from a discrete FE model as described below.

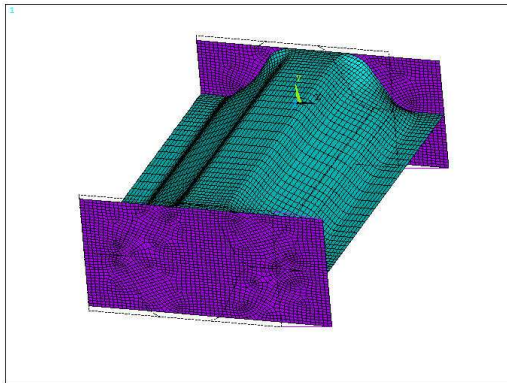


Figure 5: Displacement plot from the Finite Element model showing the thickness effect (the effect that the face sheet and cell depth have on the in-plane deformation). The top and bottom of core has the same displacement as the face sheet, while the core towards the center of the cell is less restrained.

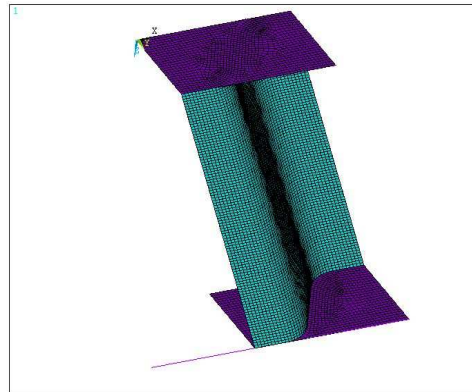


Figure 6: Discrete Finite Element model in pure shear for calculation of G_{xz}

The continuum properties are calculated directly from a discrete unit-cell FE model. These continuum properties are found by displacing the discrete model in either pure shear or extension, extracting reaction forces, then using these forces, the strain and overall dimensions of the unit-cell to compute the modulus. The in-plane modulus is found by displacing the model by a prescribed amount with the facesheets attached – and using the reaction forces from the core only and to compute the modulus.

Constraint equations were used to force the core into pure shear for the calculation of the shear moduli and to hold the sidewalls upright.

3. RESULTS

Seventeen different configurations, most of them based around standard Nomex cores with glass and carbon faces were used in this test. As the whole parameter conversion process is done within the FE package no experimental continuum properties were used. Figure 7 and Table 2 show direct comparisons between the discrete and continuum wrinkling stresses for a range of panel configurations. There is a 2.3% average difference between the discrete and continuum models for the majority of the cases, verifying that there is no difference between the wrinkling stresses predicted by the discrete and continuum models. This is a significant finding, as both models have completely different element types. The only thing that unites them is the conversion of the properties within the conversion models. With this level of correlation it is safe to use a continuum core to represent this failure mode. It also shows that the type of core chosen would not account for the observed difference between the experimental and wrinkling model results.

| Run Number | Discrete Properties | | | | | | | Calculated continuum properties | | | | | Results | |
|------------|---------------------|-------|-------|-------|-------|-------|-------------------------|---------------------------------|----------|----------|-------|-------|-----------------|------------------|
| | l | t_f | t_s | E_f | E_s | t_c | internal θ angle | E_z | G_{xz} | G_{yz} | E_x | E_y | Stress discrete | Stress continuum |
| | (mm) | (mm) | (mm) | (MPa) | (MPa) | (mm) | | (MPa) | (MPa) | (MPa) | (MPa) | (MPa) | (MPa) | (MPa) |
| 1 | 1.92 | 0.47 | 0.048 | 25500 | 3811 | 25.5 | 64.2 | 142.9 | 28.5 | 16.4 | 1.69 | 1.37 | 350.6 | 347.6 |
| 2 | 1.92 | 0.2 | 0.048 | 25500 | 3811 | 25.5 | 64.2 | 142.9 | 28.5 | 16.4 | 1.69 | 1.37 | 265.2 | 344 |
| 3 | 1.92 | 0.6 | 0.048 | 25500 | 3811 | 25.5 | 64.2 | 142.9 | 28.5 | 16.4 | 1.69 | 1.37 | 368.7 | 354.7 |
| 4 | 1.92 | 0.8 | 0.048 | 25500 | 3811 | 25.5 | 64.2 | 142.9 | 28.5 | 16.4 | 1.69 | 1.37 | 388.7 | 371.5 |
| 5 | 5.75 | 0.47 | 0.048 | 25500 | 3811 | 25.5 | 64.2 | 47.6 | 9.6 | 5.5 | 0.07 | 0.06 | 141 | 155.3 |
| 6 | 3.83 | 0.47 | 0.048 | 25500 | 3811 | 25.5 | 64.2 | 71.3 | 14.3 | 8.3 | 0.22 | 0.19 | 206.9 | 202.4 |
| 7 | 7.66 | 0.47 | 0.048 | 25500 | 3811 | 25.5 | 64.2 | 35.8 | 7.3 | 4.2 | 0.03 | 0.02 | 98.8 | 131 |
| 8 | 1.92 | 0.47 | 0.048 | 40000 | 3811 | 25.5 | 64.2 | 142.9 | 28.5 | 16.4 | 1.69 | 1.37 | 423.6 | 409 |
| 9 | 1.92 | 0.47 | 0.048 | 72000 | 3811 | 25.5 | 64.2 | 142.9 | 28.5 | 16.4 | 1.69 | 1.37 | 533.9 | 510.3 |
| 10 | 1.92 | 0.47 | 0.048 | 48750 | 4406 | 25.5 | 64.2 | 165.2 | 33 | 19 | 1.96 | 1.59 | 499.9 | 481.9 |
| 11 | 1.92 | 0.47 | 0.048 | 25500 | 5000 | 25.5 | 64.2 | 187.5 | 37.4 | 21.6 | 2.22 | 1.8 | 410.7 | 414.4 |
| 12 | 1.92 | 0.47 | 0.048 | 25500 | 8000 | 25.5 | 64.2 | 300 | 59.9 | 34.5 | 3.56 | 2.88 | 549.8 | 563.1 |
| 13 | 1.92 | 0.47 | 0.048 | 25500 | 3811 | 10 | 64.2 | 143.6 | 28.8 | 16.6 | 1.69 | 1.37 | 383.1 | 372.5 |
| 14 | 1.92 | 0.47 | 0.048 | 25500 | 3811 | 15 | 64.2 | 143.2 | 28.6 | 16.5 | 1.69 | 1.37 | 362 | 356.9 |
| 15 | 1.92 | 0.47 | 0.048 | 25500 | 3811 | 30 | 64.2 | 142.8 | 28.5 | 16.4 | 1.69 | 1.37 | 349.9 | 347 |
| 16 | 1.92 | 0.47 | 0.02 | 25500 | 3811 | 25.5 | 64.2 | 59.2 | 11.9 | 6.8 | 0.13 | 0.11 | 195 | 184.3 |
| 17 | 1.92 | 0.47 | 0.06 | 25500 | 3811 | 25.5 | 64.2 | 179.2 | 35.7 | 20.6 | 3.19 | 2.54 | 411.2 | 414 |

Table 2: Comparison of wrinkling stresses for the two different model types

Comparison between discrete and continuum models

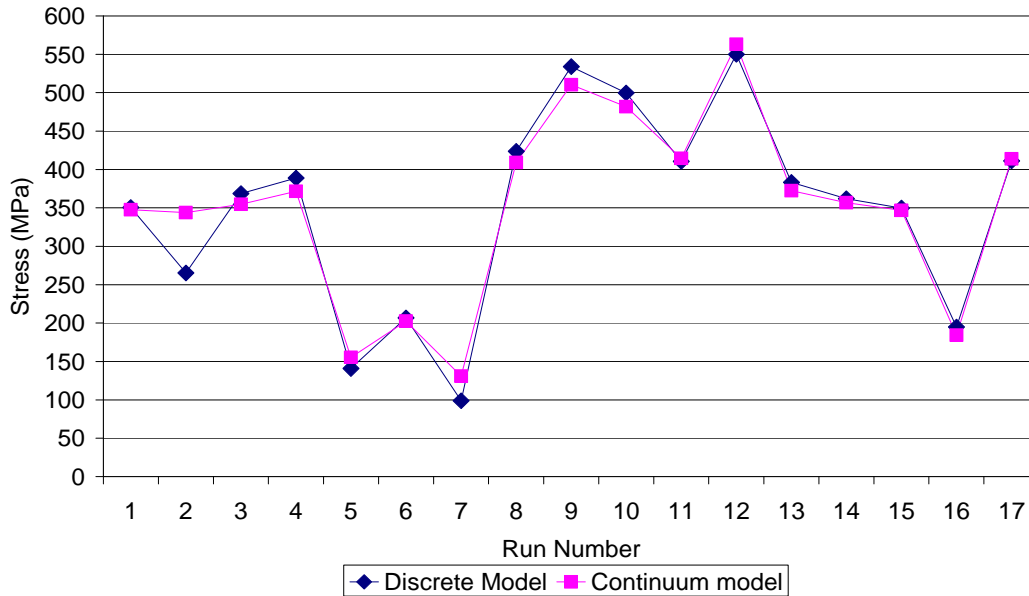


Figure 7: Comparison of wrinkling stresses for the two different model types

In models 2, 5, and 7 (Table 2) there is no direct correlation between the wrinkling stresses. In these cases a second failure mode appears, producing a difference as high as 20%. This failure mode is a combination of wrinkling and dimpling that the authors have termed ‘wrinkling/dimpling failure’. In this buckling mode the cell walls remain vertical and a localised dimple forms inside each cell at the trough of each wrinkle. With this failure mode the dimpling component absorbs some of the energy, which is otherwise used to form the wrinkle in the face sheet and bend the cellular walls. To get a wrinkling wavelength which is in the order of one cell width, the core must be much stiffer than the face sheet. In normal situations this failure mode is unlikely to occur as thin face sheets are never used on relatively dense cores, or cores with large cell sizes. This dimpling and wrinkling failure modes are shown in Figure 8 and Figure 9.

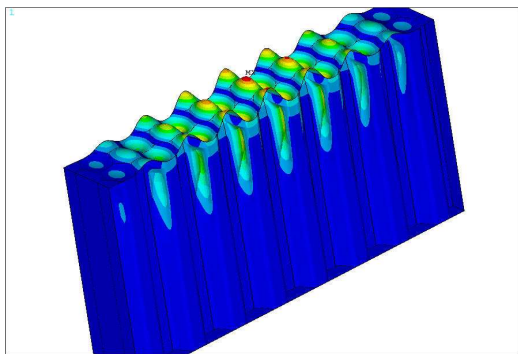


Figure 8: Wrinkling / dimpling failure mode. Occurs when the wrinkle wavelength is approximately equal to the natural wavelength

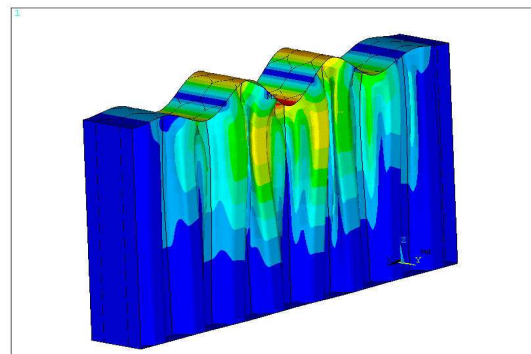


Figure 9: Wrinkling failure mechanism. Occurs when the wrinkle wavelength is greater than the cell width. This is the most common mode in a typically manufactured panel

4. COMPARISON OF THE WRINKLING STRESS PREDICTED BY FE AND ANALYTICAL MODELS

The purpose of this study was to compare the wrinkling stresses and buckling modes predicted by discrete and continuum cored models.

To add to this study the two continuum Finite Element models were compared to existing analytical expression of [6]

$$\sigma_{cr} = 0.825 \left(E_f E_z G_{xz} \right)^{\frac{1}{3}} \quad (2)$$

As discussed in the pervious Section, the in-plane modulus of the core material can have a significant effect on the wrinkling stress. This is the one property that is omitted from many classical expressions. With the current analytical model the in-plane extension terms are excluded from the derivation - this is similar to assuming that there is minimal deformation in the in-plane direction. To get the same effect in the Finite Element model, the in-plane stiffness must be large enough to stop any in-plane movement.

Table 3 shows a comparison between the wrinkling stresses predicted by the three different models.

| Properties (MPa / mm) | | | | | | | Wrinkling Stress (MPa) | | |
|-----------------------|-------|-------|----------|----------|-------|-------|------------------------|--------------------|-----------------------|
| t_c | t_f | E_f | G_{xz} | G_{yz} | E_z | E_x | analytical model | Plane stress model | Solid continuum model |
| 25.53 | 0.47 | 25500 | 28.5 | 16.4 | 142.9 | 4.2 | 388 | 383 | 363 |
| 25.53 | 0.2 | 25500 | 28.5 | 16.4 | 142.9 | 4.2 | 388 | 376 | 365 |
| 25.53 | 0.6 | 25500 | 28.5 | 16.4 | 142.9 | 4.2 | 388 | 388 | 365 |
| 25.53 | 0.8 | 25500 | 28.5 | 16.4 | 142.9 | 4.2 | 388 | 399 | 372 |
| 25.53 | 0.47 | 25500 | 9.6 | 5.5 | 47.6 | 2.7 | 187 | 192 | 183 |
| 25.53 | 0.47 | 25500 | 14.3 | 8.3 | 71.3 | 3.0 | 244 | 246 | 234 |
| 25.53 | 0.47 | 25500 | 7.3 | 4.2 | 35.8 | 2.6 | 155 | 161 | 154 |
| 25.53 | 0.47 | 40000 | 28.5 | 16.4 | 142.9 | 4.2 | 451 | 445 | 424 |
| 25.53 | 0.47 | 72000 | 28.5 | 16.4 | 142.9 | 4.3 | 548 | 544 | 520 |
| 25.53 | 0.47 | 48750 | 33.0 | 19.0 | 165.2 | 4.9 | 530 | 524 | 499 |
| 25.53 | 0.47 | 25500 | 37.4 | 21.6 | 187.5 | 5.5 | 465 | 459 | 434 |
| 25.53 | 0.47 | 25500 | 59.9 | 34.5 | 300.0 | 8.7 | 636 | 630 | 591 |
| 25.53 | 0.47 | 25500 | 539 | 310 | 2698 | 68 | 2751 | 2832 | 2429 |
| 10 | 0.47 | 25500 | 28.8 | 16.6 | 143.6 | 9.0 | 390 | 419 | 383 |
| 15 | 0.47 | 25500 | 28.6 | 16.5 | 143.2 | 6.4 | 389 | 399 | 372 |
| 30 | 0.47 | 25500 | 28.5 | 16.4 | 142.8 | 3.8 | 388 | 379 | 360 |
| 25.53 | 0.47 | 25500 | 11.9 | 6.8 | 59.2 | 1.3 | 216 | 209 | 201 |
| 25.53 | 0.47 | 25500 | 35.7 | 20.6 | 179.2 | 6.0 | 451 | 450 | 424 |

Table 3: Comparison of different wrinkling models

The plane stress FE model predicts almost identical wrinkling stresses to the analytical model (equation (2)), except in the instance where the thickness/height ratio of the sandwich is reduced. This is because the analytical model assumes that there is no interaction between the top and the bottom faces. The most notable difference is between the plane stress and the solid continuum FE models. The wrinkling stress of the solid continuum FE model is approximately 15% lower than the plane stress FE model, due to the different element formulations. There are two reasons for this. Plane stress solid elements are stiffer than three dimensional higher order elements, due to their missing degree of freedom in the depth direction. The face sheets are also made from shell elements in the solid model, which are more flexible than equivalent solid elements with the same thickness.

From these findings it was concluded that the wrinkling stress in the modified analytical model closely matches the wrinkling stress in the plane stress FE model when the correct restrained in-plane modulus was used.

It is likely that the stress values using the analytical model and the plane stress model are too high, and the most accurate linear wrinkling stress is predicted by the solid continuum model. With the solid continuum model, there is no plane stress assumption and the result also closely matches the discrete FE model, which is most representative of the linear buckling load. However, a good estimate of the linear buckling stress is still found from any of the plane stress models.

Despite the validation of the models, linear stresses are not representative of the expected experimental wrinkling stresses. When non-linear models are used, stresses are generally about 10-20% lower than these values. This type of model takes into account initial perturbations in the structure. The stresses are further reduced by premature fracturing and crushing of the core before the structure reaches the wrinkling stress. This is the actual cause of the error between the experimental and existing linear wrinkling models. The only way to accurately capture the wrinkling stress and failure stress due to wrinkling is to adopt a non-linear scheme or account for core crushing in the linear analytical model [6].

5. CONCLUSION

This study has found that a simplified continuum FE model predicts the same wrinkling stress as an equivalent discrete FE model. The agreement between the two models was very good considering the only properties that tie them together are those effective continuum properties extracted from discrete data. There was one case when the models predicted different wrinkling stresses. This was when the wrinkling wavelength approaches the cell size, in which case a discrete model is needed to capture an additional dimpling mode. The close agreement between the continuum and discrete models verifies that any discrepancy between the experimental and analytical models cannot be attributed to core representation. The significance of this finding means that continuum cores can be used to capture localised failure in discrete honeycomb panels, thus removing the need to model complex cellular geometry.

It was also shown that the analytical model of [6]

$$\sigma_{cr} = 0.825(E_f E_z G_{xz})^{\frac{1}{3}} \quad (3)$$

that excludes the in-plane modulus, offers a good estimation of the linear wrinkling stress. This is assuming that the restrained in-plane modulus (modulus calculated with face sheet attached) is used and the model is being compared with an equivalent plane stress model.

NOTATION

| Notation | Unit | Property |
|-------------------|------|---|
| G_{xz}, G_c | MPa | core shear modulus in the loading direction |
| E_z, E_c | MPa | core modulus in the out-of-plane direction |
| G_{yz} | MPa | core shear modulus perpendicular to loading direction |
| E_x | MPa | In-plane modulus in the loading direction |
| t_f | mm | facesheet thickness. |
| t_c | mm | Sandwich panel thickness |
| E_f | MPa | facesheet modulus |
| σ_{cr} | MPa | critical wrinkling stress |
| P_{cr} | N | critical wrinkling load |
| l | mm | cell wall length |
| t_s | mm | cell wall thickness |
| E_s | MPa | cell wall modulus |
| P | MPa | Maximum graduated pressure load |
| I | MPa | eigenvalue which is equivalent to P, when P is set to 1MPa |
| C | | constant that varies between 0.5 and 0.9 |
| ν_f | | Poisson ratio of the facesheet |
| ν_{zx}, ν_c | | Poisson ratio of the core in the out-of-plane loading direction |

REFERENCES

1. Plantema FJ. Sandwich Construction. Oxford: Pergamon Press; 1966.
2. Hoff NJ, Mautner SE. Buckling of sandwich type panels. Journal of Aeronautical Sciences 1945;12(3):285-297.
3. Gough E, Bruyne D, Elam C. The instability of a thin sheet by supporting medium. Journal of the Royal Aeronautical Society 1940;44(1):12-43.
4. Allen HG. Analysis and design of structural sandwich panels. Oxford: Pergamon Press; 1969.
5. Zenkert D. An introduction to sandwich Construction: Solihull; 1995.
6. Staal RA. PhD Thesis: Failure of sandwich honeycomb panels in bending [PhD]. Auckland: Department of Mechanical Engineering, University of Auckland; 2006.
7. Staal RA, Horrigan DPW, Mallinson G, Jayaraman K. Predicting failure loads of impact damaged sandwich panels. Submitted to J. Sandwich Structures and Materials 2006.
8. Gibson LJ, Ashby MF. Cellular Solids: Structure and Properties. 2 ed. UK: Cambridge University Press; 1997.
9. Burton WS, Noor AK. Assessment of continuum models for sandwich panel honeycomb cores. Computational Methods in Applied Mechanics and Engineering 1997;145:341-360.
10. Vonach WK, Rammerstorfer FG. The effects of in-plane core stiffness on the wrinkling behavior of thick sandwiches. Acta Mechanica 2000;141:1-10.